

# Creation of room-temperature DMS carbon-incorporated ZnO

A. A. DAKHEL\*

*Department of Physics, College of Science, University of Bahrain, P.O. Box 32038, Kingdom of Bahrain*

Carbonated ZnO (ZnO-C) nanocrystallite samples were prepared by sol-gel method using sucrose as a carbon ions source. The conditions including hydrogenation to create dilute magnetic semiconducting (DMS) behaviour were determined. The structural, optical and magnetic properties of ZnO-C system were systematically studied. The structural properties were studied by X-ray diffraction (XRD) and the optical properties were studied by diffuse reflection spectroscopy (DRS). It was concluded that the hydrogenation of ZnO-C samples could create O-vacancies and toss the C ion-species to drop into O-vacancies and thus could switch-on DMS properties. Therefore, ZnO-C can be used in applications of tailored magnetic properties.

(Received October 20, 2019; accepted February 15, 2021)

*Keywords:* Zinc-carbon oxide, C-incorporated ZnO, Creation of DMS

## 1. Introduction

Zinc oxide (ZnO) is one of transparent conducting oxides (TCO). It can be used as a room temperature dilute magnetic semiconductor (RT-DMS), in addition to its known optical properties with a direct optical band (~3.4 eV), degenerate semiconducting and other TC properties [1,2]. The physical properties of ZnO could be controlled by controlling its native defects like oxygen vacancies ( $V_{\text{O}}$ ) and Zn interstitials ( $Zn_{\text{i}}$ ). One of the techniques used for controlling the point defects is by inclusion/doping of impurity ions. However, the insertion of impurities could create some exotic properties, like ferromagnetic (FM). Usually, doping of ZnO with transition metal (TM) ions is used to create stable ferromagnetic (FM) properties forming ZnO-based DMS [3-9]. Pan et al [10] have theoretically and experimentally studied RT-FM in C-doped ZnO (ZnO-C) films and they obtained a magnetic moment of  $2.02 \mu_{\text{B}}/\text{C}$  when proposed that C ions substitute O ions in host ZnO crystal. The FM was supposed to be created by indirect C-C super-exchange (via structural oxygen) interactions mediated by holes. Peng et al. [11] generalized the hole-induced FM to include  $d^0$  ZnO ( $d^0$ -FM). Some Authors [12] mentioned that the FM in ZnO could be derived by native defects such as Zn interstitials or O vacancies and, thus it was proposed that the dopants in ZnO play no essential role in carrying magnetic moment. In general, the mechanism of creation of FM properties in ZnO-C based materials is complicated under more consideration. In this research, the conditions of creation of RT-FM in C-doped ZnO nanoparticles prepared by facial co-precipitation method were reported.

## 2. Experimental materials and synthesis

Carbonated ZnO (ZnO-C) nano composites were prepared by using two starting complexes; Zn acetylacetonate dihydrate (Zn-acac)  $[\text{Zn}(\text{CH}_3\text{COO})_2(\text{H}_2\text{O})_2]$  and refined sucrose ( $\text{C}_{12}\text{H}_{22}\text{O}_{11}$ ) as a source of carbon ion (from Sigma-Aldrich products). The method of the synthesis included thermal decomposition of Zn-acac in carbon environment of sucrose. Therefore, controlled amounts of Zn-acac and sucrose were merged together in ~20 mL of acetone and water mixture in a ceramic cup. The solution was magnetically stirred at room temperature (RT) for ~1h., before the temperature was raised slowly to ~60°C until a white dense gel was formed on the bottom of the beaker. The gel in the ceramic cup covered with Al foil was flash sintered in static air at 500°C/1h followed by slow cool in the closed furnace to the RT. The formed powder (ZnO-C) of mass ration C/Zn ~ 0.7 was found to be of host ZnO structure. Undoped ZnO powder was synthesised by the same procedure for comparison. In addition; some amount of the synthesised powder was annealed in hydrogen ( $\text{H}_2$ ) atmosphere at 400°C for 1h and referred as ZnO-C-H. Undoped ZnO and hydrogenated ZnO-H were prepared as references. All the prepared samples were pelletized for characterisation.

The X-ray diffraction (XRD) method used for structural analysis was carried out by a Rigaku Ultima-IV diffractometer (Cu anode). The optical properties over the range 200–1000 nm were studied by the. The diffuse reflection spectroscopy (DRS) method used for optical properties analysis was carried out by a Shimadzu UV-3600 spectrophotometer equipped with an integrating sphere. The vibrating sample magnetometer (VSM) method used for the magnetic behaviour analysis was carried out by a PMC MicroMag-3900 over the range  $\pm 10$  kOe at a step of 25 Oe/1s at RT.

### 3. Result

#### 3.1. Structural characterisation

Fig. 1 presents XRD patterns of the synthesised ZnO, ZnO-C and ZnO-C-H. It reveals hexagonal structure of all studied samples.

The diffraction peaks were indexed according to the standard JCPDS no.00-036-1451 data card of lattice parameters  $a=3.2498$  and  $c=5.2066$  Å.

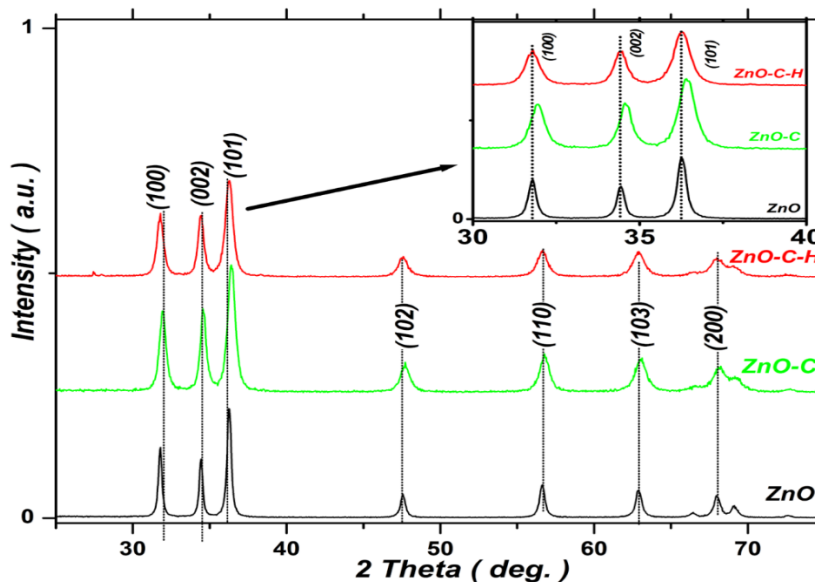


Fig. 1. XRD patterns of the synthesised samples. The inset shows the magnified 30°-40° region (color online)

The structural analyses were carried out with the Rietveld refinement and Williamson-Hall (W-H) methods, which are the components of the XR built-in PDXL software. The results are tabulated in the table:1. The values of two of the Rietveld parameters;  $R_{wp}$  (%) (weighted profile) and  $S$  (goodness-of-fit) mentioned in table:1 were acceptable since  $S$  was found in-between 1 and 2 [13]. Data

onto the Table 1 show that the average nano CS in synthesised ZnO nanocomposite was reduced by ~40% due to the carbonation. The unit-cell volume ( $V_{cell}$ ) of host ZnO slightly increased from carbonations, which disclosed the inclusion of C ions in ZnO lattice. The increasing of  $V_{cell}$  of host ZnO-C by hydrogenation is attributed to the creation of O-vacancies.

Table 1. Crystallite size (CS), lattice parameters ( $a, c, V_{cell}$ ), micro-structural strain ( $\epsilon$ ), Rietveld fitting parameters ( $R_{wp}$ ,  $S$ ) and band gap of pristine, carbonated, and hydrogenated ZnO

Sample	CS(nm)	Lattice parameters		$V_{cell}(\text{Å}^3)$	$\epsilon$ (%)	$R_{wp}(\%)$	$S$	$E_g(\text{eV})$
		$a(\text{Å})$	$c(\text{Å})$					
ZnO	29.8	3.2485	5.2053	47.570	0.29	12.76	1.175	3.23
ZnO-H	32.9	3.2483	5.2040	47.550	0.29	10.79	1.270	3.23
ZnO-C	17.5	3.2487	5.2065	47.587	0.46	13.31	1.247	3.12
ZnO-C-H	16.9	3.2496	5.2072	47.620	0.60	12.48	1.282	3.12

The experimental results can be used to study the effect of carbonation on ZnO lattice. At first, the opportunity for substitution of structural  $\text{Zn}^{2+}$  (of radius 0.074nm) by  $\text{C}^{4+}$  ions (of radius 0.016[14]) is unlikely to happen, since the radii difference is ~ 78%, which, if occurred, could strongly disturb the crystalline structure of host ZnO. Moreover, the host ZnO unit cell would, also, be destroyed with the substitution of structural  $\text{O}^{2-}$  by  $\text{C}^{4+}$  ions due to a large ionic radius of  $\text{C}^{4+}$  (0.26 nm[15,16]). Therefore, the carbonation could be occurred mainly by the occupation of  $\text{C}^{s+}$  ion-species (of diverse oxidation numbers,  $s < 4$ ) interstitial positions and lattice-point vacancies in ZnO lattice, in

addition to the possible accumulation on the crystallite boundaries (CBs). Moreover, the electronegativity required that the incorporated C to be more attracted to one structural O-ion and becoming the nearest neighbour by forming C-O bonds [17].

The hydrogenation of pristine ZnO would not create appreciable O-vacancies and therefore cannot create a measurable crystallographic and optical changes (table:1). However, the inserted C species in ZnO lattice (ZnO-C) slightly catalyzed the dissociation of  $\text{H}_2$  molecules during the hydrogenation [18]. The formed H ions/atoms are chemically active and can create O-vacancies by removing

structural oxygen. Moreover, the hydrogenation assisted the diffusion of C species throughout the ZnO lattice by tossing them and can drop them into O-vacancies. The tossing of C species throughout the ZnO lattice increased the internal strain  $\varepsilon\%$  in host ZnO (table:1). Moreover, the hydrogenation increased the unit-cell size ( $V_{\text{cell}}$ ) of host ZnO-C that usually attributed to the generation of O-vacancies.

### 3.2. Optical characterisation

The optical properties of the synthesised pristine and carbonated ZnO nanocomposite samples were studied by standard diffuse reflectance spectroscopy (DRS). The measured DR,  $R(\lambda)$  in the range of 250 – 750 nm, were used to calculate the spectral Kubelka-Munk (K-M) absorption function,  $F(\lambda)$  by;  $F(\lambda) = (1-R)^2/2R$  [19]. As shown in the inset of fig.2, the high- $\lambda$  side of spectral  $F(\lambda)$  has long hump

due to C inclusion in the samples and attributed to the creation of conduction-band traps tail.

As the function  $F(\lambda)$  is proportional to linear absorption coefficient,  $\alpha$ , then it is possible to use it to find band gap,  $E_g$  through Tauc technique [20];

$$(F \times E)^2 = B (E - E_g) \quad (1)$$

where  $B$  is the sample's constant. The direct optical band gap can be estimated from the plot  $(F \times E)^2$  vs.  $E$  following the Tauc extrapolation technique, as shown in Fig. 2 and Table 1. For undoped ZnO, the optical bandgap found (3.23 eV) is agreed with previously known values [21]. Thus, the carbonation of ZnO caused a slight band-gap redshift. Such results approved that the inclusion of C in the lattice of host ZnO reduced the concentration of conduction electrons ( $N_{el}$ ), according to Moss-Burstein (B-M) mechanism [22].

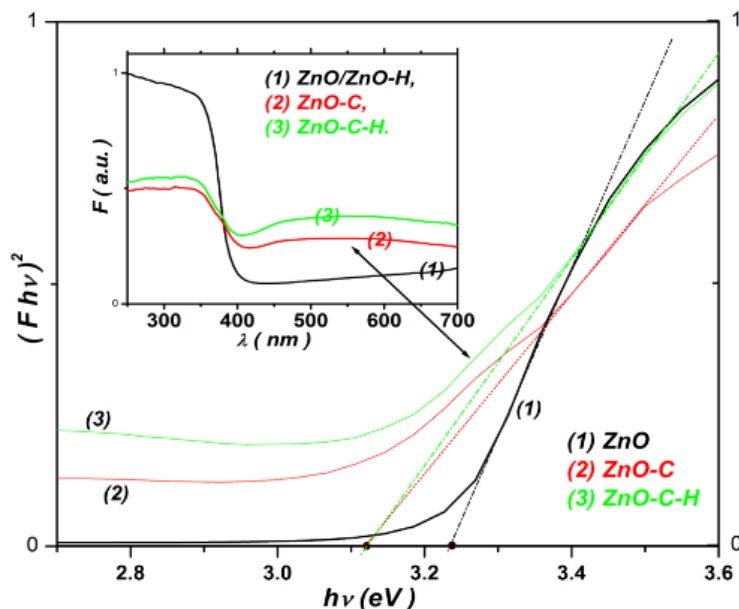


Fig. 2. Tauc plot for the synthesised samples. The inset shows the spectral K-M absorption function;  $F(\lambda)$  of the synthesised samples (color online)

### 3.3. Magnetic characterisation

The investigations show that all the synthesised pristine and carbonated ZnO powders have diamagnetic (DM) properties. Furthermore, the hydrogenation could not create RT-FM properties in pristine ZnO. However, RT-FM properties were created in hydrogenated-carbonated ZnO (ZnO-C-H). These results are attributed to the occupation of O-vacancies by dopant C ion-species as consequences of hydrogenation.

To test the effect of C-concentration, another ZnO sample doped with lower relative C concentration with mass ratio C/Zn~0.4 was synthesized by same procedure. However, that ZnO-C sample showed DM properties before and after hydrogenation. Therefore, the concentration of C

environment has critical (vital) effect on the creation of RT-FM, together with the hydrogenation. Thus, the hydrogenation is necessary to create RT-FM in carbonated ZnO but not sufficient. The created RT-FM properties became considerable and measurable for concentrations of C inclusion that is necessary to conduct the  $S.S$  interaction by direct C-C interaction or super-interaction via O-vacancies.

As shown in Fig. 3, the magnetic behaviour of ZnO-C-H demonstrated RT-FM hysteresis in addition to a partial DM behaviour. By using the built-in program, the RT-FM parameters of the magnetic hysteresis loop were obtained as follows:  $M_s = 3.83$  memu/g,  $M_r = 0.55$  memu/g,  $H_c = 185.6$  Oe.

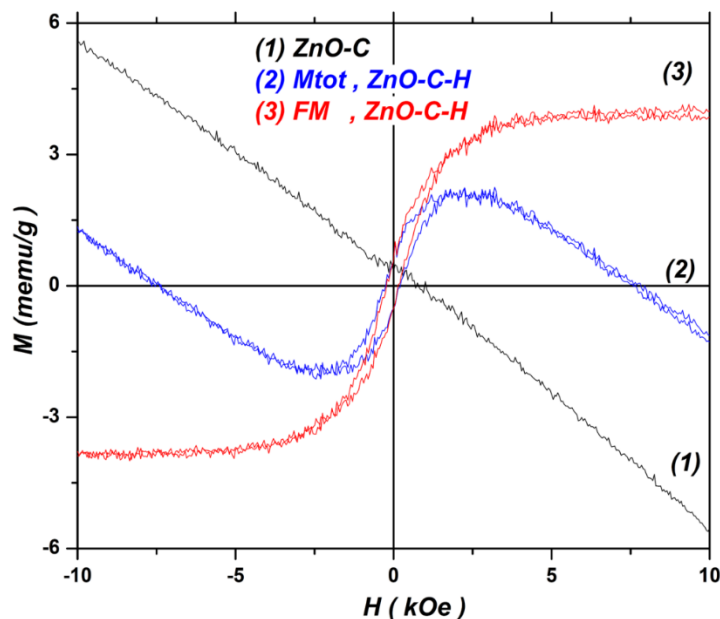


Fig. 3. Magnetic behaviour of ZnO-C and the RT-FM behaviour of ZnO-C-H sample (color online)

If we consider C<sub>2p</sub> localised magnetic moment of Carbon  $\sim 2.02 \mu_B/C$  dopant [10], then the small  $M_s$  value measured in the present investigation revealed very little amount ( $10^{-3}\%$ ) of used C ion-species participated in RT-FM interaction. It means that little amount of C ion-species that incorporated into ZnO lattice could occupy the right crystallographic position in ZnO-C-H crystal, while the major part of used C were accumulated in amorphous form on the crystallite boundaries and on interstitials. The incorporation of C species by substitution strongly influenced the growth parameters of host ZnO crystal so that the value of  $V_{cell}$  became the highest.

In summary, the hydrogenation of ZnO-C created O-vacancies and tossed the C ion-species to drop into the created O-vacancies, especially on the skin layer of the nano-crystallites. The resulting magnetic moment might be due to the substituted C-C superexchange interaction *via* O-vacancies.

#### 4. Conclusions

Crystalline nanocomposite carbonated ZnO was synthesis for DMS studies. The structural studies show that the average nano CS was reduced by  $\sim 40\%$  by carbonation of host ZnO. The volume  $V_{cell}$  of the host ZnO slightly increased from carbonation and hydrogenation, which was attributed to the formation of O-vacancies. The magnetic measurements show that the pristine and carbonated ZnO have DM properties. RT-FM was created in hydrogenated-carbonated ZnO (ZnO-C-H). This result is attributed to the occupation of created O-vacancies by dopant C ion-species as result of hydrogenation. The H<sub>2</sub>-molecules toss the dopant C ion-species to drop them into the created O-vacancies, especially on the skin layer of nano-crystallites. The long-range magnetic indirect super-exchange

interaction between C-C ion species via oxygen vacancies created RT-FM.

#### References

- [1] Nguyen Duc Dung, Cao Thai Son, Pham Vu Loc, Nguyen Huu Cuong, Pham The Kien, Pham Thanh Huy, Ngo Ngoc Ha, *J. Alloys Compds.* **668**, 87 (2016).
- [2] T. Dietl, H. Ohno, F. Matsukura, J. Cibert, D. Ferrand, *Science* **287**(5455), 1019 (2000).
- [3] D. Karmakar, S. K. Mandal, R. M. Kadam, P. L. Paulose, A. K. Rajarajan, T. K. Nath, A. K. Das, I. Dasgupta, G. P. Das, *Phys. Rev. B* **75**, 144404 (2007).
- [4] C. Song, K.W. Geng, F. Zeng, X.B. Wang, Y. X. Shen, F. Pan, Y. N. Xie, T. Liu, H. T. Zhou, Z. Fan, *Phys. Rev. B* **73**, 024405 (2006).
- [5] S. Zhou, Q. Xu, K. Potzger, G. Talut, R. Grotzschel, J. Fassbender, M. Vinnichenko, J. Grenzer, M. Helm, H. Hochmuth, M. Lorenz, M. Grundmann, H. Schmidt, *Appl. Phys. Lett.* **93**, 232507 (2008).
- [6] P. Sharma, A. Gupta, K. V. Rao, F. J. Owens, R. Sharma, R. Ahuja, J. M. O. Guillen, B. Johansson, G. A. Gehring, *Nat. Mater.* **2**(10), 673 (2003).
- [7] C. S. Wei, S. P. Lau, M. Tanemura, M. Subramanian, Y. Akaike, *Appl. Surf. Sci.* **258**(14), 5486 (2012).
- [8] M. Bououdina, A. A. Dakhel, A. Jaafar, J. H. Dai, Y. Song, *J. Alloys Compds* **776**, 575 (2019).
- [9] A. A. Dakhel, *Appl. Phys. A* **123**, 214 (2017).
- [10] H. Pan, J. B. Yi, L. Shen, R. Q. Wu, J. H. Yang, J. Y. Lin, Y. P. Feng, J. Ding, L. H. Van, J. H. Yin, *Phys. Rev. Lett.* **99**, 127201 (2007).
- [11] H. Peng, H. J. Xiang, S. H. Wei, S. S. Li, J. B. Xia, J. Li, *Phys. Rev. Lett.* **102**, 017201 (2009).
- [12] X. Zhang, Y. H. Cheng, L.Y. Li, H. Liu, X. Zuo,

- G. H. Wen, L. Li, R. K. Zheng, S. P. Ringer, *Phys. Rev. B* **80**, 174427 (2009).
- [13] L. B. McCusker, R. B. Von Dreele, D. E. Cox, D. Louer, P. Scardi, *J. Appl. Cryst.* **32**, 36 (1999).
- [14] R. D. Shannon, *Acta Crystallogr. Sect. Found. Crystallogr. A* **32**, 751 (1976).
- [15] S. Zhou, Q. Xu<sup>1</sup>, K. Potzger, G. Talut, R. Grötzschel, J. Fassbender, M. Vinnichenko, J. Grenzer, M. Helm, H. Hochmuth, M. Lorenz, M. Grundmann, H. Schmidt, *Appl. Phys. Lett.* **93**, 232507 (2008).
- [16] S. Xu, X. Sun, Yu Zhao, Y. Gao, Yi Wang, Q. Yue, B. Gao, *Appl. Surf. Sci.* **448**, 78 (2018).
- [17] Sung Sakong, Peter Kratzer, *Semicond. Sci. Technol.* **26**(1), 014038 (2011).
- [18] J. Beheshtian, A. A. Peyghan, Z. Bagheri, *J. Molecular Modeling* **19**(1), 255 (2013).
- [19] A. E. Morales, E. S. Mora, U. Pal, *Revista Mexicana de Fisica S* **53**(5), 18 (2007).
- [20] J. Tauc, F. Abelesn (ed.), *Optical Properties of Solids*, 1969, North Holland.
- [21] E. F. Keskenler, S. Dogan, B. Diyarbakir, S. Duman, B. Gurbulak, *J. Sol-Gel Sci. Technol.* **60**, 66 (2011).
- [22] J. I. Pankove, *Optical Processes in Semiconductors*, 36 (1975), Dover, NY.

---

\* Corresponding author: adakhil@uob.edu.bh